

## ARTICLE



# Fluvastatin sensitizes pancreatic cancer cells toward radiation therapy and suppresses radiation- and/or TGF- $\beta$ -induced tumor-associated fibrosis

Debasish Mohapatra<sup>1,2</sup>, Biswajit Das<sup>1,3</sup>, Voddu Suresh<sup>1,4</sup>, Deepti Parida<sup>1,4</sup>, Aliva Prity Minz<sup>1,4</sup>, Usharani Nayak<sup>5,4</sup>, Amlan Priyadarshree Mohapatra<sup>1,4</sup>, Rajeeb K. Swain<sup>5</sup> and Shantibhusan Senapati<sup>1</sup>✉

© The Author(s), under exclusive licence to United States and Canadian Academy of Pathology 2021, corrected publication 2021

Pancreatic cancer (PC) is highly resistant to chemo and radiotherapy. Radiation-induced fibrosis (RIF) is a major cause of clinical concern for various malignancies, including PC. In this study, we aimed to evaluate the radiosensitizing and anti-RIF potential of fluvastatin in PC. Short-term viability and clonogenic survival assays were used to evaluate the radiosensitizing potential of fluvastatin in multiple human and murine PC cell lines. The expression of different proteins was analyzed to understand the mechanisms of fluvastatin-mediated radiosensitization of PC cells and its anti-RIF effects in both mouse and human pancreatic stellate cells (PSCs). Finally, these effects of fluvastatin and/or radiation were assessed in an immune-competent syngeneic murine model of PC. Fluvastatin radiosensitized multiple PC cell lines, as well as radioresistant cell lines *in vitro*, by inhibiting radiation-induced DNA damage repair response. Nonmalignant cells, such as PSCs and NIH3T3 cells, were less sensitive to fluvastatin-mediated radiosensitization than PC cells. Interestingly, fluvastatin suppressed radiation and/or TGF- $\beta$ -induced activation of PSCs, as well as the fibrogenic properties of these cells *in vitro*. Fluvastatin considerably augmented the antitumor effect of external radiation therapy and also suppressed intra-tumor RIF *in vivo*. These findings suggested that along with radiation, fluvastatin co-treatment may be a potential therapeutic approach against PC.

*Laboratory Investigation* (2022) 102:298–311; <https://doi.org/10.1038/s41374-021-00690-7>

## INTRODUCTION

Pancreatic ductal adenocarcinoma (PDAC) is one of the most aggressive human malignancies, with only 8% patients showing 5-year survival<sup>1</sup>. For most patients with PC, the condition is diagnosed at the late stage of cancer progression; hence only 15–20% patients are eligible for surgery<sup>2,3</sup>, and chemotherapy and radiation therapy (RT) are the only treatment options available for patients with late-stage PC. Although radiotherapy has been used in both adjuvant and neoadjuvant settings in patients with PC, but only 20% patients show a noteworthy response<sup>2</sup>. Hence, identification of novel therapeutic approaches that may sensitize pancreatic cancer cells (PCCs) toward RT is urgently required.

Irrespective of malignancies, RT not only damages proliferating tumor cells, but also induces unwanted injury and radiation-induced fibrosis (RIF), which contributes significantly to morbidity<sup>4</sup>. Fibrotic or desmoplastic stroma is a hallmark of PDAC and is known to promote tumor progression and non-responsiveness to chemotherapy, RT, and immunotherapy<sup>5</sup>. Radiation-induced tissue injury of both tumor and non-tumor tissues trigger inflammation, which further stimulates recruitment and trans-differentiation of fibroblasts into myofibroblasts<sup>6</sup>. The activated myofibroblasts produce excessive extracellular matrix (ECM) proteins such as collagen and fibronectin, which contribute to RIF<sup>4,6</sup>. Several

studies have evaluated the anti-fibrotic efficacy of various drug candidates<sup>4,7</sup>. However, the number of approved therapies for RIF remains insignificant. Hence, a rational combination of drugs that may sensitize PCCs towards radiation and/or suppress RIF is of paramount clinical significance.

Different pathways have been proposed to be involved in the radiosensitization process<sup>8</sup>. Certain metabolic regulators of PCCs are known to control the response to RT in PC<sup>9,10</sup>. The cholesterol and fatty acid synthesis pathways have been implicated as important regulators of radioresistance in PCCs<sup>11</sup>. In addition to their cholesterol-limiting effects, statins or 3-hydroxyl-3-methyl glutarate-coenzyme A reductase inhibitors also possess anti-inflammatory, immunomodulatory, anti-oxidant, and cytotoxic properties<sup>12</sup>. Multiple studies have shown radiosensitizing effects of statins in different malignancies<sup>13–15</sup>. At the same time, statins such as pravastatin have been found to be effective against RIF in humans and animals<sup>16,17</sup>. Although different statins have been investigated for their radiosensitizing effect in diverse malignancies, studies regarding the effect of fluvastatin (a lipophilic statin) as a radiosensitizer on malignancies are lacking.

Accumulating clinical and experimental evidence indicates that the beneficial effects of statins are beyond their cholesterol-lowering effects<sup>12</sup>. Their effects on ionizing radiation (IR)-induced

<sup>1</sup>Tumor microenvironment and animal models lab, Institute of Life Sciences, Bhubaneswar, Odisha, India. <sup>2</sup>School of Biotechnology, KIIT University, Bhubaneswar, Odisha, India. <sup>3</sup>Manipal Academy of Higher Education, Manipal, Karnataka, India. <sup>4</sup>Regional Centre for Biotechnology, Faridabad, Haryana, India. <sup>5</sup>Vascular Biology lab, Institute of Life Sciences, Bhubaneswar, Odisha, India. ✉email: [senapati@ils.res.in](mailto:senapati@ils.res.in)

Received: 5 July 2021 Revised: 16 October 2021 Accepted: 18 October 2021

Published online: 12 November 2021

DNA damage and regulation of autophagy and apoptosis have been reported earlier, and autophagy could be a pro-survival strategy for cells<sup>18,19</sup>. Recent studies have also shown a close relationship between autophagy and apoptosis<sup>20</sup>. Hence, the effect of statins on autophagy and their role in IR-induced cell death warrants investigations.

In this study, we examined the effect of fluvastatin on radiation response. We further investigated the effect of fluvastatin on RIF and TGF- $\beta$ -mediated activation of fibroblasts. Taken together, our data suggests repurposing fluvastatin as a potential radiosensitizer for pancreatic cancer.

## MATERIALS AND METHODS

### Cell culture

Human PCC lines (MiaPaCa-2, BxPC3, and AsPC-1) were purchased from the European Type Culture Collection. The mouse PCC line, UN-KC-6141, was a kind gift from Dr. S K Batra, UNMC, USA,<sup>21</sup> and the mouse embryonic fibroblast cell line (NIH3T3) was a kind gift from Dr. Soumen Chakraborty, Institute of Life Sciences, India. MiaPaCa-2, AsPC1, UN-KC-6141, and NIH3T3 cells were cultured in Dulbecco's modified Eagle's medium (DMEM), and BxPC3 was cultured in Roswell Park Memorial Institute (RPMI)-1640 medium supplemented with 10% fetal bovine serum (FBS) and 1% penicillin/streptomycin in a humidified incubator at 37 °C in the presence of 5% CO<sub>2</sub>. The cells were checked for *Mycoplasma* contamination in every 3 months. The short tandem repeat profiles of all cancer cell lines were confirmed by the institutional sequencing facility. With the prior approval of the Institutional Animal Ethical Committee (IAEC) (ILS, Bhubaneswar, India), mouse primary pancreatic stellate cells (PSCs) were isolated from C57BL/6 mice by adopting methods already standardized in our lab<sup>22</sup>. Human primary PSCs were procured from ScienCell Research Laboratories and cultured with 2% FBS containing Stellate Cell Medium (SteCM; ScienCell). All the primary PSCs were used between passage numbers 2–4.

### Radiation

The cultured cells were irradiated with the indicated dose of X-rays using the precision X-ray machine (X-RAD 225). The cells were placed 5 cm from the focus and the irradiation rate was 1.5 Gy/min.

### Cell viability assay

Crystal violet assay was used as a standard technique to evaluate the ability of the molecules to radiosensitize PC cells. Briefly, 3000 cells were seeded in individual wells of a 24-well plate in triplicate and incubated with fluvastatin (5  $\mu$ M or as indicated) for 6 h before radiation (2 Gy or as indicated). After 18 h of radiation (24 h of treatment), drug-supplemented media was replaced by normal media and the cells were cultured for 72 h (further 48 h). After incubation, the cells were fixed with formalin and stained with 0.05% crystal violet solution. The stained plates were dried and images were captured. For quantification, the crystal violet stain was dissolved in 10% acetic acid and absorbance was measured at 540 nm on Varioskan<sup>TM</sup> Flash multimode reader (Thermo Scientific).

### Colony-forming assay

MiaPaCa-2, BxPC3, AsPC-1, and UN-KC-6141 cells ( $0.5 \times 10^3$ ) were seeded in 35 cm<sup>2</sup> cell culture plates. After 24 h of seeding, the cells were treated with fluvastatin 6 h before radiation and followed by different doses of radiation. The fluvastatin-treated medium was replaced after 18 h of radiation and the cells were cultured for 5 days, after which the colonies were fixed with formalin and stained with crystal violet solution (0.05%). Colonies containing  $\geq 50$  cells were counted. Subsequently, the survival fraction (SF) was calculated.

### Establishment of radioresistant cell line

MiaPaCa2 cells were exposed to 2 Gy radiations daily for 5 days followed by taking 2 days off (giving a total of 10 Gy fractionated dose/week). This challenge was repeated for 3 weeks to give a total of 30 Gy fractionated dose. Throughout the radiation process and recovery time, cells were kept at 50–70% confluency to ensure potential for exponential growth. After completion of third week of radiation, cells were maintained in media containing 10% FBS, washed and retreated with fresh media for next 2 weeks without radiation. Radioresistance property was verified by

comparing the radiosensitivity of radiation selected cells with their parental cell lines by colony-forming assay.

### Preparation of pancreatic stellate cell (PSC)-conditioned medium (PSC-CM)

Human PSCs ( $20 \times 10^3$ ) were seeded into 25 cm<sup>2</sup> TC-flask and cultured in stellate cell medium for 24 h, followed by treatment with 5  $\mu$ M fluvastatin. After 24 h of fluvastatin treatment, the media was changed and the cells were washed with phosphate buffered saline (PBS). Then, fresh media was added and the cells were allowed to grow for another 24 h. The culture medium was collected and centrifuged at 1500 rpm, 4 °C, for 30 min. The supernatant was collected as conditioned medium (CM) and stored at  $-80$  °C until further use.

### Immunoblotting

After appropriate duration of treatment, the cultured cells were washed twice with PBS and protein lysates were prepared using radio-immunoprecipitation assay buffer (20 mM Tris-HCl (pH 7.5), 150 mM NaCl, 1 mM Na<sub>2</sub>EDTA, 1 mM EGTA, 1% NP-40, 1% sodium deoxycholate, 2.5 mM sodium pyrophosphate, 1 mM beta-glycerophosphate, 1 mM Na<sub>3</sub>VO<sub>4</sub>, and 1  $\mu$ g/mL leupeptin) containing a phosphatase inhibitor and a protease inhibitor. Protein isolation, estimation, and immunoblotting were performed as described previously<sup>23</sup>. All the antibodies used for immunoblotting are mentioned in Supplementary Table 1. Densitometric quantification of the protein bands were carried out by using the Image J program (NIH). The intensity of each protein band in a blot was normalized to the intensity of the corresponding  $\beta$ -actin band. For each blot, fold change in protein expression was calculated by dividing the protein density of each condition by the corresponding control sample. For each protein, results are presented as the mean of the fold change and standard deviations obtained from minimum three independent experiments.

### Flow cytometry analysis

The level of apoptosis was evaluated using Annexin-V and 7-aminoactinomycin D (7-AAD) double staining with BD FACS Accuri<sup>15</sup>.

### Immunofluorescence

Cells, grown on glass coverslips for 24 h, were treated with fluvastatin (5  $\mu$ M) for the indicated time points, followed by irradiation with 2 Gy. After 6 or 24 h of radiation, the cells were fixed and permeabilized with acetone:methanol (1:1) for 10 min at  $-20$  °C. Then, the cells were washed with 1 $\times$  PBS and blocked with 5% bovine serum albumin. The cells were incubated with phospho- $\gamma$ H2AX (1:200) or LC3-II antibody overnight at 4 °C. The coverslips were then incubated with Alexa Fluor-conjugated secondary antibodies (1:500) for 1 h at room temperature in dark and mounted with 4', 6-diamidino-2-phenylindole (DAPI). The fluorescence images were captured using Apotome.2 (ZEISS) and a confocal microscope (STED, Leica).

### In vivo tumor model

The animal experiments were performed with prior approval from the IAEC, Institute of Life Sciences, Bhubaneswar, India. C57BL/6 mice were maintained according to the guidelines of the IAEC and irradiated using a Precision-250 X-Ray radiator operating at 160 kV and 25 mA at the dose rate of 1.5 Gy/min. C57BL/6 mice, subcutaneously injected with UN-KC-6141 cells ( $2 \times 10^6$ ) in 100  $\mu$ L PBS developed growing tumors within 6–8 days. Fluvastatin and RT were started once the tumor volume reached 250–300 mm<sup>3</sup> on day 11. For combination treatment, mice were treated with fluvastatin (15 mg/kg) via oral gavage 1 h before radiation (15 Gy per mouse). In individual treatment groups, mice received fluvastatin (15 mg/kg) or 15 Gy radiation per mice. Mice received four doses of fluvastatin (total 60 mg/kg) and four doses of fractionated radiation (total 60 Gy). Mice were administered only PBS in the untreated group. Before irradiation, all the animals were anesthetized and lead blocks were arranged above the body, leaving only the tumor area on hind flank for the treatment. The animals were sacrificed on the 4th day of the last radiation dose. BrdU (100 mg/kg body weight) was injected 1 h before sacrifice to label the proliferating cells.

### Tissue processing and immunohistochemistry (IHC)

Tissue samples were collected and preserved in 10% buffered formalin solution at room temperature. For histopathological analysis, tissues were processed for paraffin embedding, and multiple 5-micron sections were prepared. Hematoxylin and eosin staining were performed as described previously<sup>22</sup>. IHC was performed to detect Ki67, BrdU, and  $\alpha$ -SMA following

the procedures described earlier<sup>22,23</sup> and the dilution of the primary antibodies are mentioned in Supplementary Table 1. Trichrome staining<sup>22</sup> was used to detect the level of collagen deposition. Images were captured using a microscope (Leica ICC50 HD) and the staining was quantified using the ImageJ software.

**Hydroxyproline assay**

Frozen KC tumor tissues were homogenized using a mortar pestle and lyophilized. Furthermore, collagen content was estimated following the instruction provided with the hydroxyproline assay kit (Sigma; MAK008).

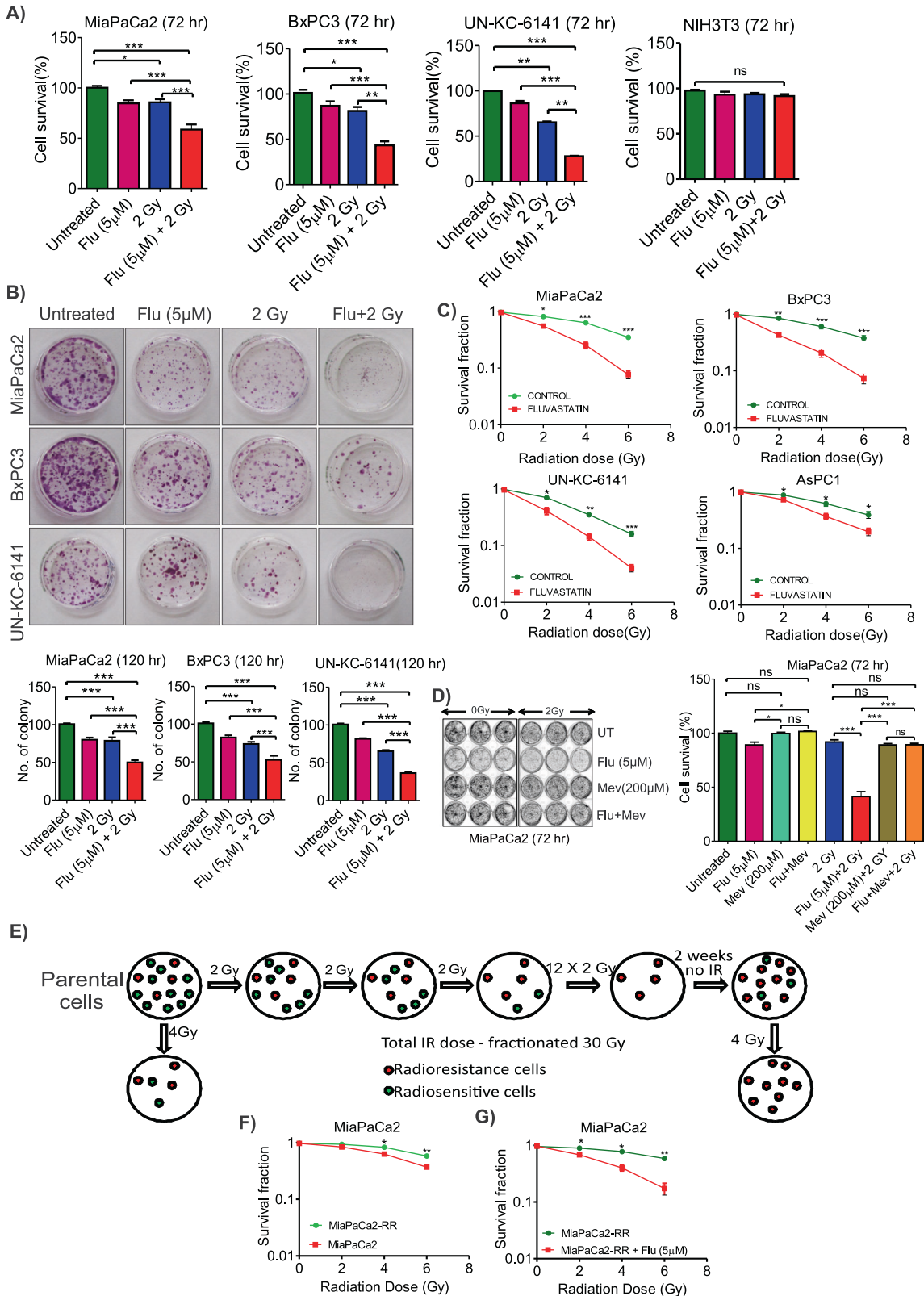


**Fig. 1 Fluvastatin enhanced radiosensitivity in pancreatic cancer cells in vitro.** **A** The bar graphs represent the percentage of survival calculated from the crystal violet assay (72 h). The data show mean  $\pm$  SEM.  $n = 3$ ,  $*p < 0.05$ ,  $**p < 0.005$  and  $***p < 0.001$ . **B** Images showing representative crystal violet-stained plate in colony-forming assay. The bar graphs below the images represent quantification of the results of the colony-forming assay (5 days post-radiation). The data show mean  $\pm$  SEM.  $n = 3$ ,  $***p < 0.001$ . **C** The line graphs show the reduction in SF of different cell lines upon co-treatment with radiation and fluvastatin, calculated from the results of the colony-forming assay (5 days post-radiation). The data show mean  $\pm$  SEM.  $n = 3$ ,  $*p < 0.05$ . Survival fraction = No. of colony (irradiated)/No. of colony (nonirradiated). **D** The crystal violet-stained plate images and corresponding quantification graphs showing rescue of fluvastatin-mediated cell death upon mevalonate supplementation.  $*p < 0.05$ ,  $**p < 0.005$ ,  $***p < 0.001$ ;  $n = 3$ . **E** Schematic representation of the method used to generate the radioresistant MiaPaCa2 cell line (MiaPaCa2-RR). The detailed method is described in Materials and method. **F** Line graph showing the reduced sensitivity of the MiaPaCa2-RR cells to radiation. The data represents quantification of the results of the colony-forming assay (5 days post-radiation).  $n = 3$ ,  $*p < 0.05$ . **G** Line graph presenting the survival fraction shows the reduced viability of MiaPaCa2-RR cells upon co-treatment with fluvastatin (Flu) and radiation. The data represents quantification of the results of the colony-forming assay (5 days post-radiation).  $n = 3$ ,  $*p < 0.05$ .

## In vivo zebrafish model

**Embryo collection and maintenance.** Experiments related to zebrafish embryos were performed at the institutional zebrafish facility at ILS (approved by CPCSEA, Government of India). The experiment was performed using 24 h post fertilization (hpf) to 120 hpf zebrafish embryos. Zebrafish wild-type strain, Tübingen (TÜ), was used to check the effect of fluvastatin after radiation treatment. Fertilized embryos were collected at one or two-celled stage and were maintained in  $1 \times E3$  embryo medium (5 mM NaCl, 0.17 mM KCl, 0.33 mM  $MgSO_4$ , 0.33 mM  $CaCl_2$ , and  $10^{-5}\%$  methylene blue) under normoxic conditions at  $28.5^\circ C$ <sup>24</sup>. The embryos were staged according to Kimmel et al.<sup>25</sup>.

**Radiation dose standardization.** At 24 hpf, 15 healthy embryos were taken in 35 mm Petri plates containing 2 mL E3 media and were irradiated with different doses of X ray (0, 5, 8, 10, 12, 15, and 20 Gy). After irradiation, the embryos were maintained in the incubator at  $28.5^\circ C$  till 120 hpf.

**Drug and radiation treatment.** The embryos were treated with only fluvastatin (0, 1, 2, 5, and 10  $\mu M$ ) or irradiated with 8 Gy of radiation 6 h post-drug treatment. After 24 h post-drug treatment (48 hpf), the fluvastatin-containing media was replaced with normal media, and zebrafish were maintained till 120 hpf to evaluate morphology and survival.

**Analysis of the effects of treatment on zebrafish survival and gross morphology.** Embryos at 72, 96, and 120 hpf were anesthetized with a 1:100 4 mg/mL tricaine methanesulfonate. The immobilized embryos were taken on a glass slide and their morphologies was assessed using a Leica stereo microscope (MZ16) at  $\times 32.5$  magnification. Similarly, the survival of the embryos was visually assessed till 120 hpf.

## Statistical analysis

Each experiment (except in vivo experiment) was performed thrice in triplicate and the data are presented as mean  $\pm$  SEM from a single representative experiment performed in triplicate. Comparisons between groups were evaluated using unpaired *t*-test or two-way analysis of variance (ANOVA) of GraphPad Prism 5.00 (GraphPad Software, Inc., San Diego, USA).

## RESULTS

### Fluvastatin enhanced radiosensitivity of PCCs via the mevalonate pathway

The cholesterol synthesis pathway has been reported as an important regulator of radioresistance in PCCs<sup>11</sup>. First, we planned to compare the radiosensitizing effect of statins using a short-term cell viability assay. Using the MiaPaCa2 cell line, we determined a radiation dose of 2 Gy in our initial in vitro screening. Irradiating MiaPaCa2 cells at 2 Gy followed by 72 h observation induced minimal cytotoxicity ( $\sim 20\%$ ) (Supplementary Fig. S1A), hence this assay allowed us to check the radiosensitizing effect of different statins. The radiosensitizing potential of different statins was determined using a constant dose of drugs (5  $\mu M$ ) and radiation (2 Gy). Comparison of the cytotoxic effect of drugs/radiation with the combined treatment revealed that fluvastatin acts as the most

effective radiosensitizing statin in this assay system (Supplementary Fig. S1B). Corroborating the results of previous reports, most of the statins induced cytotoxic effects in this assay<sup>26,27</sup>, and 5  $\mu M$  each of lovastatin and fluvastatin showed lesser cytotoxicity when used singly than the others (Supplementary Fig. S1B). Owing to the high cytotoxicity of many statins at 5  $\mu M$  concentration, their radiosensitizing effects could not be determined.

Further evaluation of the radiosensitizing effect of various doses of fluvastatin (from 0.1 to 10  $\mu M$ ) at a constant dose of radiation (2 Gy) showed significant radiosensitization at the minimum concentration of 3  $\mu M$  (Supplementary Fig. S1C). Up to 5  $\mu M$ , the drug itself was less cytotoxic, but showed significant radiosensitizing property. At higher concentration (10  $\mu M$ ), the drug itself was highly cytotoxic, because of which the radiosensitization effect was not noticeable (Supplementary Fig. S1C). On the basis of these data, we decided to perform the subsequent in vitro studies using 5  $\mu M$  fluvastatin. The radiosensitization effect of fluvastatin was further investigated in other PCC lines (BxPC3, AsPC1, and UN-KC-6141) and results showed significant effects in all the cell lines used (Fig. 1A, B and Supplementary Fig. S1D, E). Importantly, the nonmalignant mouse embryonic fibroblast cell line, NIH3T3, was not radiosensitized by 5  $\mu M$  fluvastatin (Fig. 1A). Furthermore, the clonogenic assay was used to analyze the SF. Results suggested that co-treatment with fluvastatin (5  $\mu M$ ) and radiation (2 Gy) significantly reduced cancer cell survival irrespective of the cell lines used (Fig. 1C,  $*p < 0.05$ ,  $**p < 0.005$ ,  $***p < 0.001$ ). To investigate whether fluvastatin-mediated radiosensitization depended on the mevalonate pathway, mevalonate (200  $\mu M$ ) was added exogenously along with fluvastatin and cell viability was determined using the crystal violet assay. Results showed significant suppression of fluvastatin-induced cytotoxicity and radiosensitization upon treatment with exogenous mevalonate (Fig. 1D). To check the radiosensitizing effect of fluvastatin on radioresistant PCCs, a radioresistant cell line (MiaPaCa2-RR) was generated (Fig. 1E). MiaPaCa2-RR was confirmed by comparing its radiosensitivity with that of its parental cell lines using the colony-forming assay. To further validate fluvastatin-mediated radiosensitization in MiaPaCa2-RR, the colony-forming assay was used to analyze the SF. Results suggested that fluvastatin treatment increased the radiosensitivity of MiaPaCa2-RR (Fig. 1F, G)

### Fluvastatin inhibited repair of radiation-induced DNA double strand damage

Radiation-induced cell death involves the formation of DNA double strand breaks (DSBs) and disruption of the DNA repair system. To determine whether fluvastatin treatment enhanced radiation-induced DNA damage and interfered with the DNA damage repair response, we performed immunofluorescence and immunoblotting and evaluated the level of phosphorylated histone H2AX (p- $\gamma$ H2AX), a sensor of DNA strand breaks and promoter of efficient DSB repairs. Both immunofluorescence (Fig. 2A, B) and immunoblot (Fig. 2C) analysis at two time points

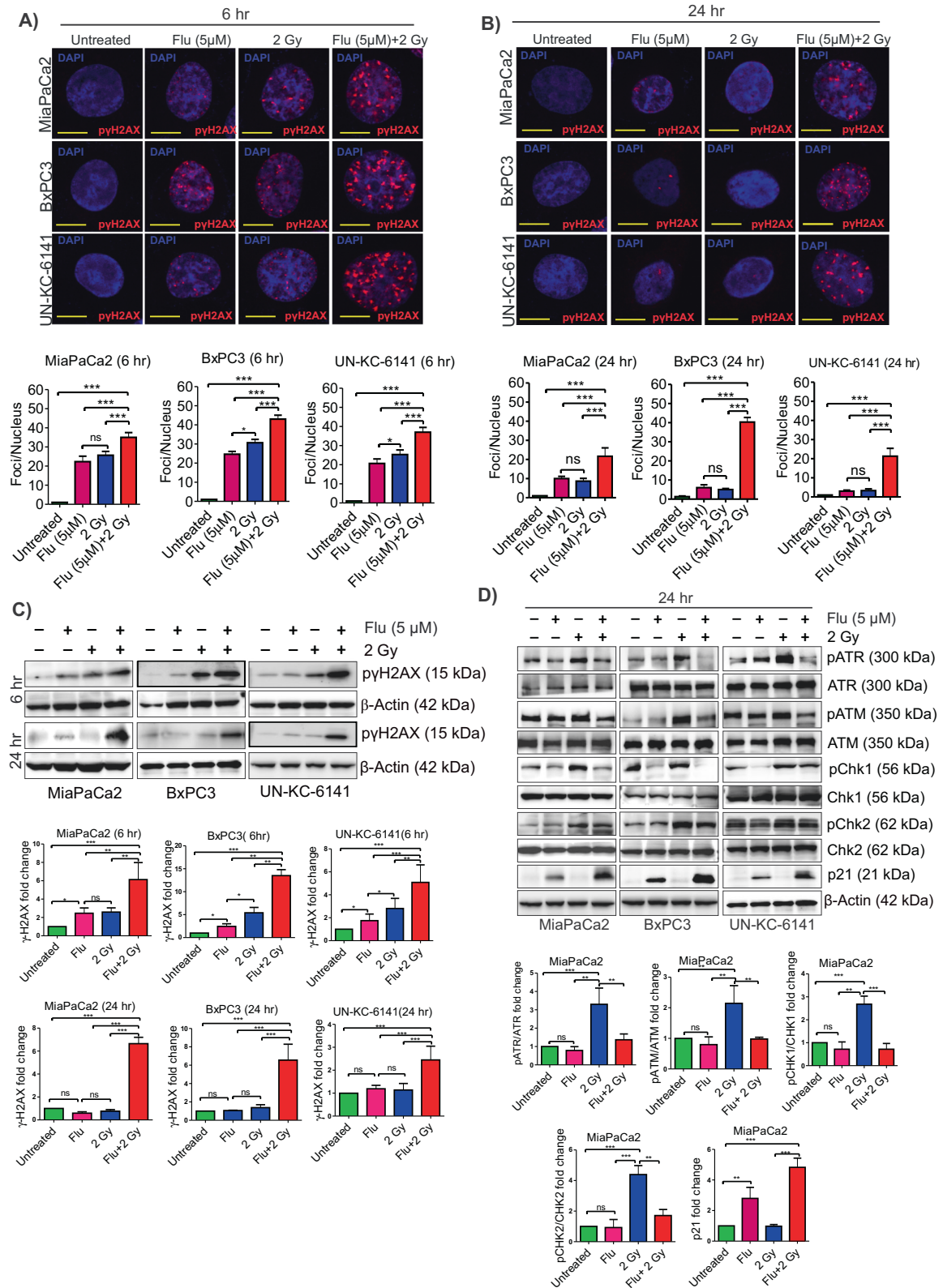


**Fig. 2** Fluvastatin suppressed repair of radiation-induced DNA double strand breaks. **A, B** Immunofluorescence images ( $\times 63$ , scale bar = 20  $\mu$ m) showing increase in nuclear (blue, DAPI) foci of phospho- $\gamma$ H2AX (red). Bar graphs below the images represent the quantification of phospho- $\gamma$ H2AX foci. Immunofluorescence staining for phospho- $\gamma$ H2AX was performed 6 h (**A**) or 24 h (**B**) after irradiation. The bar graphs below the respective panels represent the quantification of the number of phospho- $\gamma$ H2AX foci.  $n = 5$ ,  $*p < 0.05$ ,  $**p < 0.005$ ,  $***p < 0.001$ . **C** Immunoblotting showing increase in phospho- $\gamma$ H2AX level after co-treatment with fluvastatin and radiation at early (6 h) and later time point (24 h). **D** Immunoblot analysis of proteins involved in radiation-induced DNA damage repair response. The bar graphs below the western blots images (in **C, D**) are relative protein levels in MiaPaCa2 cells quantified by densitometry. Data represents the mean  $\pm$  SD ( $n = 3$ )  $*p < 0.05$ ,  $**p < 0.005$ ,  $***p < 0.001$ .

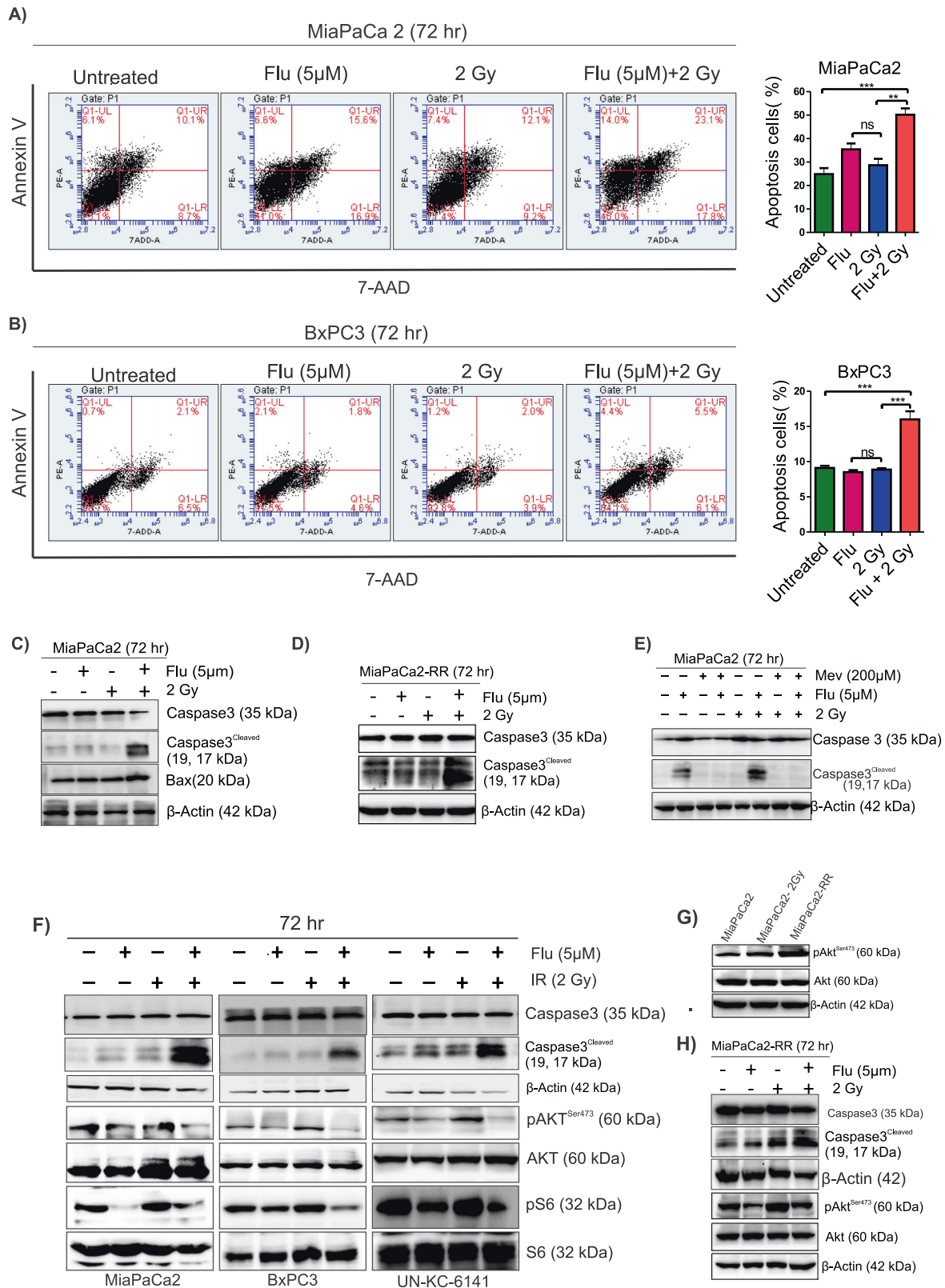


**Fig. 3** Fluvastatin enhanced radiation-induced apoptosis in pancreatic cancer cells. **A, B** Dot plot showing apoptosis assessed 72 h after treatment using FACS with Annexin V-PE/7-ADD double staining in MiaPaCa2 and BxPC3 cells pre-treated with fluvastatin. **C** Immunoblot showing elevation in apoptotic markers in MiaPaCa2 in combination treatment. **D** Immunoblot showing that fluvastatin promotes apoptosis in radioresistant MiPaCa2 (MiPaCa2-RR) to radiation. **E** Immunoblot showing that mevalonate treatment lowered the cleaved caspase3 and rescued PCCs from fluvastatin-mediated radiosensitization. **F** Immunoblot showing that inhibition of the Akt signaling pathway by fluvastatin contributed to radiosensitization. **G** Immunoblot showing increase in level of pAKT<sup>Ser473</sup> in MiaPaCa2-RR cells compared to that observed in 2 Gy-treated and untreated MiaPaCa2 cells. **H** Immunoblot showing that fluvastatin treatment promotes apoptosis in radioresistant cells (MiaPaCa2-RR) by targeting the Akt pathway.

(6 and 24 h) showed increase in phospho- $\gamma$ H2AX level upon co-treatment compared to that observed after individual treatment and no treatment at an early time point (6 h). In contrast, the phospho- $\gamma$ H2AX level decreased 24 h in individual (post-radiation or fluvastatin) treatment groups. However, the phospho- $\gamma$ H2AX

level remained elevated upon co-treatment of fluvastatin and radiation 24 h post-radiation, indicating inhibition of radiation-induced DNA damage repair response (Fig. 2B, C). Hence, to determine the effect of fluvastatin on radiation-induced DNA damage repair at the molecular level, the expression levels of

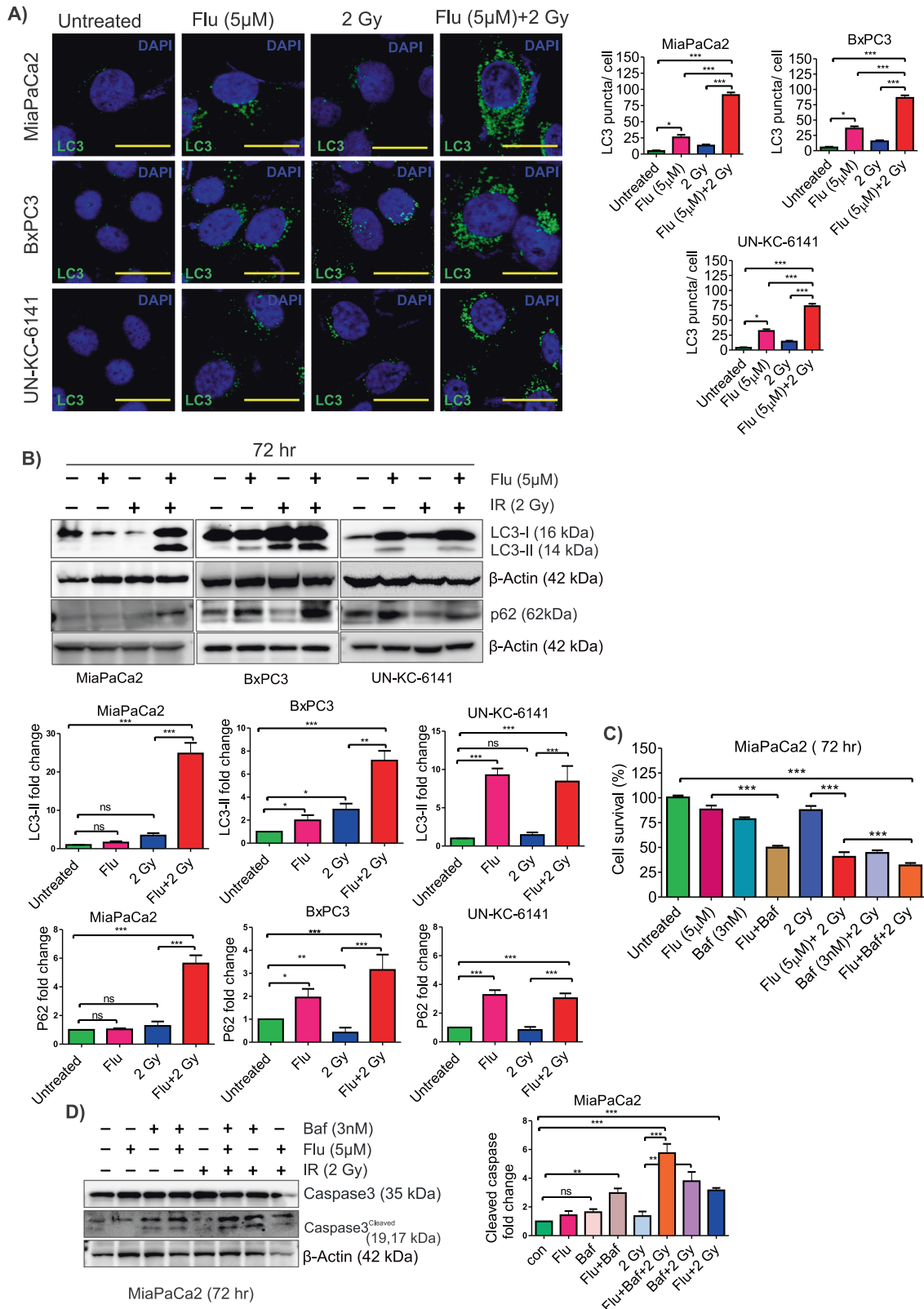


**Fig. 4 Effect of fluvastatin and radiation on autophagy in pancreatic cancer cells. A** Immunofluorescence images ( $\times 40$ , scale bar = 20  $\mu\text{m}$ ) showing increase in endogenous LC3-II puncta (green) after fluvastatin (Flu) or fluvastatin and radiation (2 Gy) co-treatment (72 h). Bar graphs below the images represent the quantification of LC3-II puncta.  $n = 10$ ,  $*p < 0.05$ ,  $***p < 0.001$ . **B** Immunoblot showing increase in LC3-II, and p62 level when the cancer cells were co-treated with fluvastatin (Flu) and radiation (IR). The bar graphs below the western blots images are relative protein levels in MiaPaCa2, BxPC3, and UN-KC-6141 cells quantified using densitometry. Data represents the mean  $\pm$  SD ( $n = 3$ )  $*p < 0.05$ ,  $**p < 0.005$ ,  $***p < 0.001$ . **C** Bar graph showing the percentage cell viability calculated from crystal violet assay in the presence or absence of bafilomycin A1 (Baf).  $n = 3$ ,  $*p < 0.05$ ,  $**p < 0.005$ ,  $***p < 0.001$ . **D** Immunoblot showing the level of cleaved caspase 3 (apoptosis marker) in the presence or absence of bafilomycin A1 (Baf). The bar graph is relative protein levels in MiaPaCa2 cells quantified using densitometry. Data represents the mean  $\pm$  SD ( $n = 3$ )  $*p < 0.05$ ,  $**p < 0.005$ ,  $***p < 0.001$ .

major DNA damage repair proteins, such as Chk-2, pChk-2, Chk-1, pChk-1, ATM, pATM, ATR, and pATR, were assessed using immunoblot analysis. We observed reduction in the level of the phosphorylated form of the above proteins in the co-treatment group compared to that in the radiation alone group, which suggested that fluvastatin inhibited DNA repair (Fig. 2D and Supplementary Fig S2A, B). Elevation in p21 level under co-treatment condition further indicated the persistence of DNA damage and inhibition of cell cycle progression (Fig. 2D and Supplementary Fig S2A, B). Together, these results suggested that fluvastatin suppressed radiation-induced DNA damage repair activity in PCCs.

#### Fluvastatin blocked the Akt signaling pathway to enhance radiation-induced cell death in pancreatic cancer cells

To further investigate the reason behind the growth inhibition induced by radiosensitization of fluvastatin in PCCs, flow cytometry and western blotting were used to determine the level of apoptosis. Apoptosis was assessed after annexin-V-PE and 7-AAD staining using flow cytometry. The result showed that 2 Gy radiation and fluvastatin alone moderately increased apoptosis in MiaPaCa2 and BxPC3 cell lines; however, pre-treatment with fluvastatin remarkably enhanced radiation-induced apoptosis in both the cell lines (Fig. 3A, B). Consistently, fluvastatin pre-treatment further increased the level of both cleaved caspase 3 and Bax in MiaPaCa2 (Fig. 3C and Supplementary Fig. S3A) and increased level of cleaved caspase 3 in MiaPaCa2-RR cells (Fig. 3D and Supplementary Fig. S3B). To investigate whether the apoptosis induced by fluvastatin-mediated radiosensitization depends on the mevalonate pathway, western blotting was used to determine the level of cleaved caspase3 after treatment with 200  $\mu\text{M}$  mevalonate. Results showed that exogenous addition of mevalonate reduced the level of cleaved caspase3 and rescued the PCCs from fluvastatin-mediated radiosensitization (Fig. 3E and Supplementary Fig. 3C). Previous studies have demonstrated that increase in Akt signaling due to radiation contributes to radioresistance in multiple cancer cell lines and that inhibition of the PI3K/Akt signaling pathway can inhibit DNA DSB repair and improve radiosensitivity<sup>28–30</sup>. Fluvastatin was also reported to inhibit the Akt signaling pathway<sup>31,32</sup>. Therefore, we speculated that fluvastatin might affect the radiosensitivity of PCCs by inhibiting the Akt signaling pathway. Western blot analysis revealed that the levels of phosphorylated Akt and phosphorylated S6 in MiaPaCa2, BxPC3, UN-KC-6141, and AsPC1 cell lines were elevated after radiation, whereas pre-treatment with fluvastatin reduced radiation-induced Akt pathway activation (Fig. 3F and Supplementary Fig. S3D–H). Consistent with this observation, cleaved caspase 3 level remained elevated in the combined treatment group (Fig. 3F and Supplementary Fig. S3D–H). Importantly immunoblot analysis showed upregulation of phospho-Akt in the radioresistant MiaPaCa2 cell line (Fig. 3G and Supplementary Fig. S3I), whereas fluvastatin treatment enhanced cleaved caspase 3 level in MiaPaCa2-RR by inhibiting radiation-induced Akt activation (Fig. 3H and Supplementary Fig. S3J). Taken together, these data demonstrated that fluvastatin enhanced the radiosensitivity of PCCs by targeting the Akt signaling pathway.

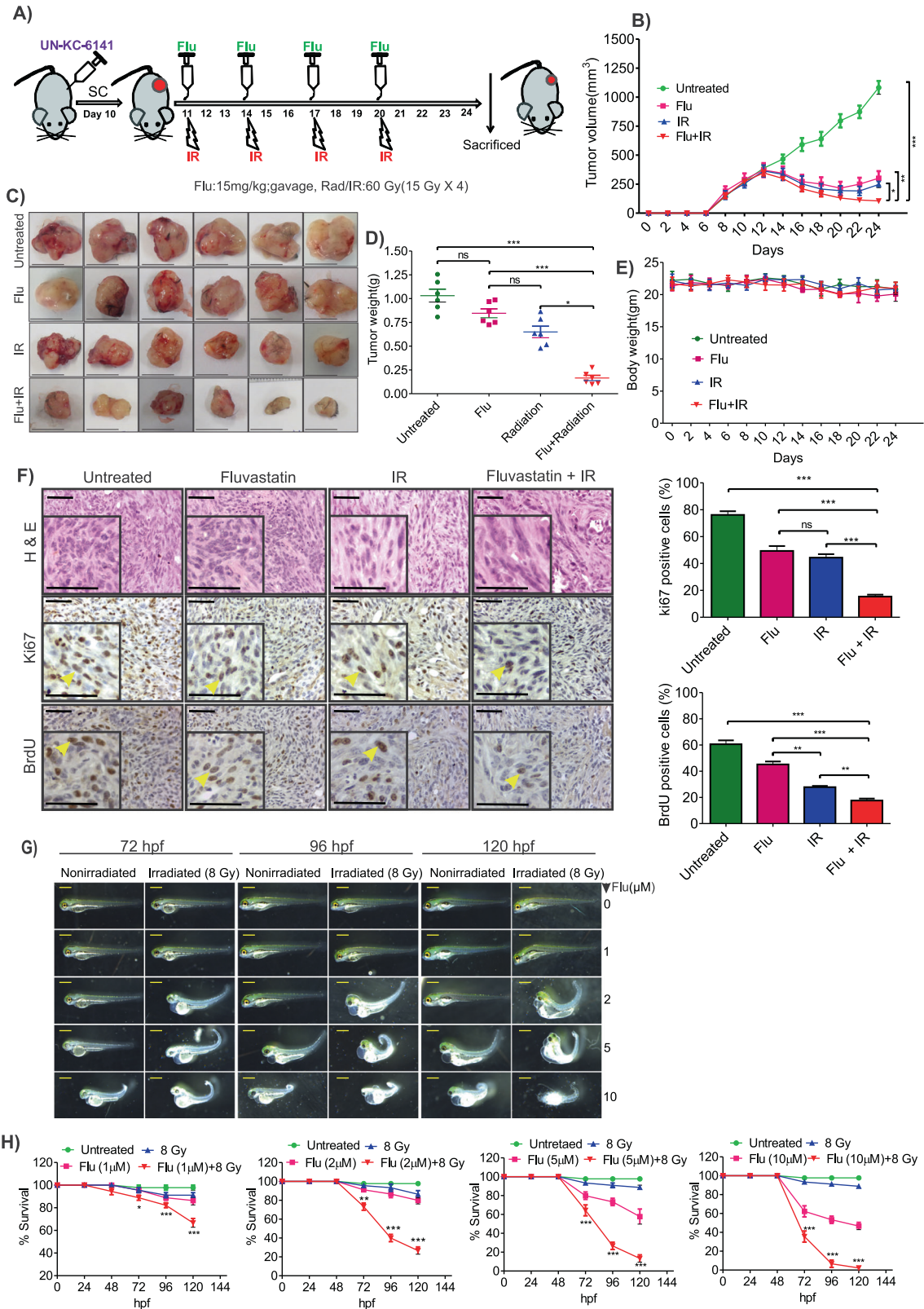
#### Fluvastatin induced autophagy and inhibited autophagy flux in pancreatic cancer cells with and without radiation

Inhibition of the Akt signaling pathway has become an attractive mechanism to increase the efficacy of chemotherapy and radiotherapy because of its involvement in autophagy, which plays a major role in chemo- and radioresistance of cancer cells<sup>33,34</sup>. Statins also act as inducers of autophagy and alter autophagy flux in different conditions<sup>35–37</sup>, therefore, to assess the status of autophagy after radiation and/or fluvastatin treatment in PCCs, the levels of LC3-I and LC3-II, markers of autophagy, were checked in different PCCs using immunofluorescence (Fig. 4A) and immunoblot analysis (Fig. 4B and Supplementary Fig. S3K). Quantification of LC3-II punctae showed significantly higher number of puncta in MiaPaCa2, BxPC3, and UN-KC-6141 cells when treated with both fluvastatin and radiation than individual treatment or no treatment (Fig. 4A). Immunoblot analysis also showed the increased LC3-II level in combination treatment (Fig. 4B). Inhibition of AKT phosphorylation, reduced level of phospho-S6 (Figs. 3F and S3D–H) and increased LC3-II punctae (Fig. 4A) suggest induction of autophagy upon fluvastatin co-treatment with IR. To further evaluate the effect of fluvastatin on autophagy flux in different PCCs, p62 protein level was evaluated through immunoblot analysis. Interestingly, fluvastatin significantly upregulated p62 level with radiation in PCCs (Fig. 4B) suggesting that autophagy flux is inhibited which could be contributing to radiosensitization and cell death. Together, fluvastatin induced increased LC3-II, p62 level and downregulated of pAkt<sup>Ser473</sup> and phospho-S6 upon co-treatment (fluvastatin and radiation) indicates induction of autophagy and inhibition of autophagic flux in PCCs. Although increase in autophagy can act as a survival mechanism in radioresistant cell lines, but some cancer cells become sensitive to radiation upon induction of autophagy<sup>27</sup>. Hence, to understand the involvement of autophagy in radiation-induced cell survival or death of PCCs, MiaPaCa2 cells were treated with a bonafide autophagy inhibitor, bafilomycin A1 and/or fluvastatin. Our observations suggested that co-treatment with bafilomycin A1 and fluvastatin enhanced cell death compared to treatment with fluvastatin alone and combination of fluvastatin and radiation (Fig. 4C). Immunoblot analysis for cleaved caspase-3 also suggested that bafilomycin A1 treatment further enhanced the radiosensitizing effect of fluvastatin in PCCs (Fig. 4D).

#### Fluvastatin enhanced the efficacy of radiation therapy in vivo

To examine the efficacy of fluvastatin as a radiosensitizer in vivo, an immunocompetent UN-KC-6141 syngeneic mouse subcutaneous pancreatic tumor model was used (Fig. 5A). Co-administration of fluvastatin and radiation significantly reduced the tumor size and tumor weight compared to that observed after individual therapies (Fig. 5B–D). The body weight of the animals did not differ significantly among groups, indicating negligible side effect of fluvastatin (Fig. 5E). Furthermore, histopathological analysis showed significantly lower number of Ki67- and BrdU-positive cells in tumor tissue sections from animals of the co-treatment group than in other conditions (Fig. 5F). The number of proliferative cells (Ki67- or BrdU-positive cells) in tumor tissues





correlated with the effect of different therapies on overall tumor growth. Taken together, our results suggested that fluvastatin enhanced the efficacy of RT in pancreatic cancer.

The in vitro findings of our study suggested that fibroblast or myofibroblast-like cells are less sensitive to fluvastatin-induced

radiosensitization than cancer cells (Figs. 1A and 6E, F). At the same time, our in vivo data did not highlight any noticeable adverse effect of fluvastatin when restricted body parts of mice (those bearing only the tumor) were exposed to radiation. However, these findings did not rule out the possible adverse

**Fig. 5 The radiosensitization effect of fluvastatin on pancreatic cancer cells in in vivo syngeneic tumor model.** **A** Schematic representation of the method used for the animal experiment. The subcutaneous tumors were irradiated as indicated (15 Gy/mice) and fluvastatin was administered orally at the dose of 15 mg/kg of body weight. **B** Graph showing reduction in tumor progression upon fluvastatin (Flu), radiation (IR), and fluvastatin + radiation treatments. Tumor volume ( $\text{mm}^3$ ) =  $\frac{1}{2} \times \text{length} \times (\text{width})^2$ .  $n = 6$ . \* $p < 0.05$ , \*\* $p < 0.005$ , \*\*\* $p < 0.001$ . **C** Digital images showing reduction in tumor size after fluvastatin treatment (scale bar = 1 cm). **D** The graph represents the tumor weight from different groups of treatment. \* $p < 0.05$ , \*\*\* $p < 0.001$ ;  $n = 6$ . **E** Graph showing the body weight of all the tumor-bearing mice throughout the experiment.  $n = 6$ . **F** Images of representative micrograph for hematoxylin-eosin, BrdU, and Ki67 immunohistochemistry ( $\times 40$ , scale bar = 50  $\mu\text{m}$ ) in different groups. The adjacent bar graph represents the quantification using the ImageJ software. \* $p < 0.05$ , \*\* $p < 0.005$ , \*\*\* $p < 0.001$ ;  $n = 5$ . **G** Bright field images of developing zebrafish embryos under indicated conditions. **H** Graphs showing the survival of zebrafish embryos in response to the indicated conditions.

effect of fluvastatin and/or radiation on other cell types of the body. Previously, statins have been implicated in alterations in embryonic development of zebrafish at morphological, physiological, and molecular levels<sup>24,32,38</sup>. Statins, tested for their anti-angiogenic potential in the zebrafish model, were also found to be effective against different types of cancer<sup>12,38</sup>. Hence, we used zebrafish (*Danio rerio*) embryos to validate the radiosensitizing effect of fluvastatin and also to assess its effect on proliferating nonmalignant cells. Initially, viable zebrafish embryos were exposed to 0–20 Gy X-ray 24 hpf, and embryos were examined for morphological changes and viability at 96 hpf. Results showed that compared to the control embryos, the irradiated ( $\leq 5$  Gy) embryos did not exhibit any morphological abnormalities, edema, and curvature of body axis; however, embryos irradiated with higher dose ( $\geq 5$  Gy) showed morphological abnormalities. Irradiation with 8 Gy led to minimal tail bending and minimum death; however, embryos that received  $\geq 10$  Gy radiation showed maximum death of embryos (Supplementary Fig. 4A). Based on these data, we picked 8 Gy dose for the final experiment assuming that any possible radiosensitizing effect conferred by fluvastatin might induce severe deformities or death at 8 Gy in zebrafish embryos. Low dose of fluvastatin alone (1 and 2  $\mu\text{M}$ ) did not induce any developmental abnormalities, whereas higher dose (5 and 10  $\mu\text{M}$ ) alone induced significant developmental abnormalities (Fig. 5G). Low dose of radiation (8 Gy) and fluvastatin (2  $\mu\text{M}$ ) synergistically affected morphological abnormalities, such as curvature of body axis, edema, and defective swim bladder development in zebrafish embryo at 72, 96, and 120 hpf (Fig. 5G). Our findings strongly indicated that fluvastatin induced radiosensitization in zebrafish embryos, as the survival percentages decreased drastically when embryos were treated with high concentration of fluvastatin and single dose of radiation (Fig. 5H). Taken together, our data suggested that fluvastatin enhanced the sensitivity of rapidly dividing cells, such as zebrafish embryonic cells and cancer cells, to radiation. Moreover, the data suggests that use of precision radiotherapy along with fluvastatin might have better clinical outcome without much normal tissue toxicity.

#### Fluvastatin impeded RIF and inhibited radiation- and/or TGF- $\beta$ -mediated fibroblasts activation

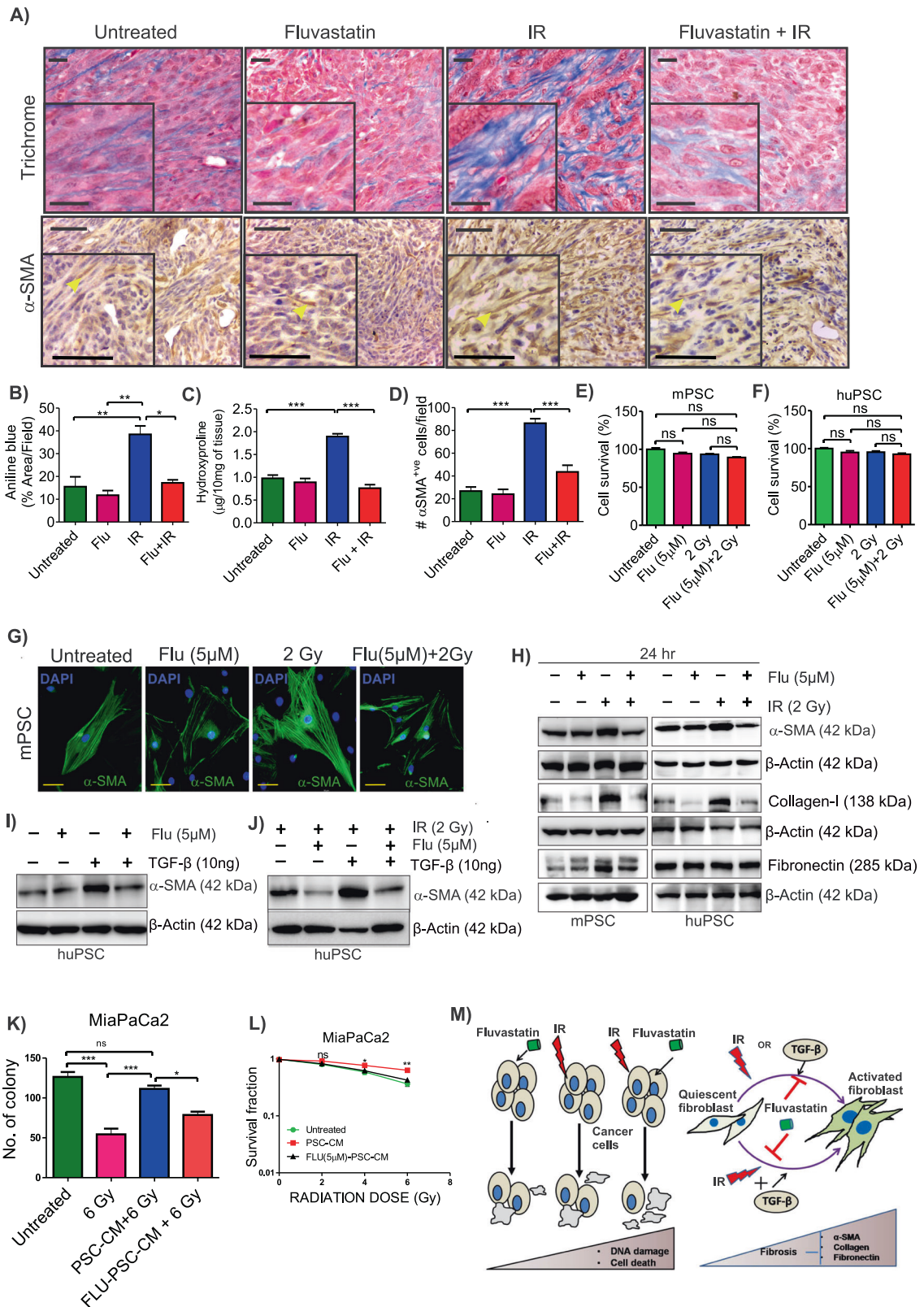
Next, we investigated the effect of fluvastatin on RIF by estimating intra-tumor collagen deposition. Our data showed significantly higher amount of collagen deposition in radiated tumors than in non-treated tumor tissues (Fig. 6A–C). Although fluvastatin itself does not significantly affect the basal level of collagen deposition in pancreatic tumors, it significantly hindered radiation-induced intra-tumor collagen deposition (Fig. 6A–C). The pancreatic tumor consists of a heterogeneous population of fibroblasts of different origins, which contributes to the intra-tumor deposition of ECM proteins such as collagen and fibronectin<sup>5</sup>. PSCs, a major contributor to the pool of pancreatic cancer-associated fibroblast cells, are known to be activated upon irradiation<sup>4</sup>. In addition to the activation of PSCs, radiation might also promote intra-tumor recruitment of myofibroblast-like cells by inducing inflammatory reactions<sup>4</sup>. Therefore, to assess the effect of fluvastatin on PSCs in

the context of radiation, we detected the number of  $\alpha$ -SMA (markers of activated PSCs) positive cells in tumor tissues of different experimental groups using IHC. Fluvastatin treatment reduced the number of  $\alpha$ -SMA positive cells in tumor tissues of the co-treated group (Fig. 6A, D). The cell viability assay confirmed that unlike that observed in cancer cells, 5  $\mu\text{M}$  fluvastatin was minimally cytotoxic for both mouse and human PSCs, and that fluvastatin did not radiosensitize these cells (Fig. 6E, F). Fluvastatin inhibited radiation-induced activation of fibroblasts, as was evident from the reduction in  $\alpha$ -SMA level in mouse PSCs (Fig. 6G, H and Supplementary Fig. S4B) and huPSCs (Fig. 6H and Supplementary Fig. 4C). Simultaneously, reduction in collagen expression was detected in both mouse and human PSCs, and reduction in fibronectin level was observed in muPSCs treated with both fluvastatin and radiation compared to radiation alone (Fig. 6H and Supplementary Fig. 4B, C).

Accumulating evidence suggests that TGF- $\beta$  is the key molecule that regulates fibroblast activation and pancreatic tumor-associated fibrosis. In our study, increased  $\alpha$ -SMA expression in huPSCs was observed upon treatment with 10 ng TGF- $\beta$  (Fig. 6I) and/or radiation (2 Gy) (Fig. 6J). Interestingly, fluvastatin (5  $\mu\text{M}$ ) reduced  $\alpha$ -SMA expression in TGF- $\beta$ -treated and/or irradiated cells (Fig. 6I, J). Previous reports have already demonstrated that stellate cells promote radioresistance of cancer cells<sup>39</sup>. To investigate the effect of PSC on radioresistance,  $0.5 \times 10^3$  MiaPaCa2 cells were cultured with PSC-CM/Flu-PSC-CM and DMEM at 1:1 ratio 24 h prior to radiation. Then, the cells were exposed to 6 Gy of cytotoxic radiation and colony number was counted after 120 h. The results showed that PSC-CM promoted radioresistance at 6 Gy, whereas fluvastatin-treated PSC-CM did not enhance radioresistance in MiaPaCa2 cells (Fig. 6K). Furthermore, colony-forming assay showed that fluvastatin inhibited PSC-mediated radioresistance (Fig. 6L). Taken together, our findings suggested that fluvastatin inhibited radiation- and/or TGF- $\beta$ -mediated fibroblast activation and inhibited PSC-mediated radioresistance in pancreatic cancer (Fig. 6M).

#### DISCUSSION

While the colony formation assay has been considered the 'gold standard' for assessing the radiosensitizing effect of different drug candidates, short-term viability assays have also shown potential for evaluating the radiosensitizing effect of targeted drug candidates<sup>40</sup>. In this study, fluvastatin was identified as a good radiosensitizer of PCCs using short-term viability assays. Previous studies have suggested that pravastatin acts as a radio-protector<sup>41</sup>. We also obtained the same result using our short-term assay system (Supplementary Fig. S1B). Together, these data reaffirmed the reliability of using short-term viability assays to assess the radiosensitizing effect of targeted drug candidates<sup>40</sup>. Although statins, such as simvastatin, atorvastatin, and lovastatin<sup>13,15</sup>, have already been reported as radiosensitizers, but the radiosensitization efficacy of fluvastatin has not been investigated in any malignancy, including pancreatic cancer. In this study, we determined the potential of fluvastatin as a radiosensitizer. We



observed that 5  $\mu$ M fluvastatin showed the best effect on the MiaPaCa2 target cell line after 24 h of drug exposure and 72 h of irradiation.

Fluvastatin is a clinically approved drug for the treatment of patients with hypercholesterolemia<sup>32</sup>. Its cytotoxic effect against

the MiaPaCa2 PCC line has been reported previously<sup>42</sup>. To the best of our knowledge, this is the first report that emphasizes the radiosensitizing efficacy of fluvastatin in any cancer. The multiple cancer cell lines of human and mouse origins and genetic backgrounds used in this study showed radiosensitization in

**Fig. 6 Fluvastatin hindered radiation-induced fibrosis and PSC-mediated radioresistance.** **A** Representative trichrome-stained micrographs showing level of collagen (aniline blue) in different groups of tumors ( $\times 40$ , scale bar = 20  $\mu\text{m}$ ). The immunohistochemistry images for  $\alpha$ -SMA are as indicated. Yellow arrow head indicates the representative stained cell for the indicated molecule ( $\times 40$ , scale bar = 50  $\mu\text{m}$ ). Quantification bar graph for aniline blue (**B**) and hydroxyproline (**C**) and  $\alpha$ -SMA (**D**).  $*p < 0.05$ ,  $**p < 0.005$ ,  $***p < 0.001$ ;  $n = 5$ . **E, F** Bar graphs showing no effect of fluvastatin (Flu) and/or radiation on the viability of mouse pancreatic stellate cells (mPSC) and human pancreatic stellate cells (huPSC). **G** Immunofluorescence images of mPSC showing reduction in the level of  $\alpha$ -SMA upon fluvastatin treatment (scale bar = 20  $\mu\text{m}$ ). **H** Immunoblot showing fluvastatin-mediated decrease in level of fibrotic molecules in mouse pancreatic stellate cells (mPSCs) and human pancreatic stellate cells (huPSC). **I** Immunoblot showing that fluvastatin inhibited TGF- $\beta$ -induced  $\alpha$ -SMA expression in human pancreatic stellate cells (huPSC). **J** Immunoblot showing that fluvastatin suppressed the effect of combination of radiation and TGF- $\beta$  on  $\alpha$ -SMA expression in human pancreatic stellate cells (huPSC). **K** Bar graph shows viability of MiaPaCa2 cells from colony formation assay indicating huPSC-mediated radioresistance (5 days post-radiation). The data show mean  $\pm$  SEM;  $n = 3$ ,  $***p < 0.001$ . **L** Line graphs showing reduction in survival fraction of MiaPaCa2 cell line upon supplementation with CM of fluvastatin-treated huPSCs compared to those treated with only CM of huPSCs (5 days post-radiation). The data presented show mean  $\pm$  SEM.  $n = 3$ ,  $*p < 0.05$ . **M** Overview of fluvastatin-mediated radiosensitization in pancreatic cancer.

presence of fluvastatin (Fig. 1A), which strongly indicated that fluvastatin might exert similar effects on different patients with PC. Previous studies have suggested that pitavastatin and other lipophilic statins are potent inhibitors of DNA DSB repair, because of which they can radiosensitize cancer cells<sup>43</sup>. Our results also demonstrated that fluvastatin delayed radiation-induced DNA DSB repair in PCCs (Fig. 2). However, the rescue of fluvastatin-induced radiosensitization of PCCs by exogenous mevalonate administration indicated the involvement of the cholesterol synthesis pathway (Fig. 1D)<sup>43</sup>. ATM-Chk2 and ATR-Chk1 pathways are frequently activated simultaneously in cells exposed to diverse genotoxic stress, including IR, and perturbations of these signaling pathways lead to cell cycle arrest and cell death<sup>44–46</sup>. Our data strongly indicated that fluvastatin inhibited IR-induced DSB repair response, as major DNA damage response proteins such as pATM, pATR, pChk2, and pChk1 were downregulated after co-treatment with fluvastatin and radiation (Fig. 2D)<sup>44</sup>. We have observed persistence of phospho- $\gamma$ H2AX foci/nucleus even after 24 h of radiation in combined treatment (Fig. 2A–C) which corroborates the previous findings for other statins<sup>13,19</sup>.

Fluvastatin has been reported as autophagy inducer, however, these studies have not investigated autophagy flux status with markers like p62<sup>20,47</sup>. Our data shows that fluvastatin enhanced both LC3-II and p62 level with and without radiation in PCCs, indicating its role as an autophagy flux inhibitor in PCCs (Fig. 4A, B). IR induces autophagy, which might exert cytoprotective or cytotoxic effects<sup>38,48,49</sup>. The findings of this study showed that autophagy inhibitor bafilomycin A1 itself radiosensitized PCCs, and co-treatment with fluvastatin and bafilomycin A1 further enhanced cell death (Fig. 4C, D). Together, these findings indicate that inhibition of autophagy flux by fluvastatin sensitizes PCCs towards radiation-induced apoptosis. A similar kind of finding has also been reported for the effect of chloroquine on bladder cancer cells<sup>50</sup>.

Our in vivo experiment suggests fluvastatin as a potential radiosensitizer (Fig. 5) corroborating in vitro experimental data. RIF is a major harmful effect of radiotherapy in most cancers<sup>4</sup>. In addition to the radiosensitization of cancer cells, fluvastatin also significantly suppressed RIF in KC tumors (Fig. 6A–D). The substantially lower number of myofibroblast-like cells ( $\alpha$ -SMA positive) and lesser deposition of collagen in tumor stroma after radiation and fluvastatin co-treatment than that observed after only irradiation might be due to the direct and/or indirect effect of fluvastatin on cancer-associated fibroblasts. The in vitro data clearly showed that without affecting the cell viability (Fig. 6E, F), fluvastatin directly suppressed the activation and fibrogenic properties of PSCs (Fig. 6G, H), a major contributor to the cancer-associated fibroblast population in pancreatic tumors<sup>5</sup>. Previously, pravastatin has been shown to exert an anti-fibrotic effect and improve radiation-induced intestinal fibrosis in rats<sup>17</sup>.

One of the major limitations of the current study is that chemotherapy was not administered in addition to fluvastatin and

radiation. Fluvastatin is known to synergistically enhance the cytotoxicity of gemcitabine in a human PC cell line<sup>42</sup>. Furthermore, our preliminary screening was done with only one concentration of different statins (5  $\mu\text{M}$ ) and radiation dose (2 Gy); hence, the potential radiosensitizing effects of other statins can't be ruled out. In this study, we have precisely irradiated subcutaneously grown murine tumor tissues, with minimal exposure to the surrounding normal tissues. This has enabled us to monitor and measure tumor growth on a daily basis. Nevertheless, this model has certain limitations. Although irradiation of only subcutaneously grown tumors has helped us address the effect of radiation and/or fluvastatin specifically on cancer cells and cancer-associated stromal cells, this method cannot be used to understand the effect of these treatments on normal tissues and organs. Moreover, we could not evaluate the effects of these treatments on the metastasis and overall survival of the control and treated animals using this model. Although the study with the mouse model of PC has demonstrated the effect of fluvastatin on suppression of RIF, its effect on other severe side effects of radiation, such as ulceration and bleeding in the stomach and intestine, are yet to be investigated. Due to the highly proliferative nature of zebrafish embryonic cells, this model has been used to evaluate different radio-sensitizers or -protectors. The effect of fluvastatin to sensitize zebrafish embryos confirms its radiosensitizing effects; however, it also raises a question about its unwanted toxic effects on highly proliferating normal cells. We believe that adoption of precision radiation techniques with fluvastatin will help to achieve better clinical outcomes without many side effects.

In conclusion, our study has provided experimental evidence that shows that fluvastatin acts as a potential radiosensitizer for pancreatic cancer by suppressing radiation-induced DNA damage repair response and inhibiting autophagic flux (Supplementary Fig. S5). Fluvastatin also exhibits a potent anti-RIF effect as it inhibits radiation/TGF- $\beta$ -induced activation of fibroblast cells. On the basis of these findings, fluvastatin might be a potential radiosensitizer and/or anti-fibrotic drug for PDAC in future (Fig. 6M).

#### DATA AVAILABILITY

All the data are available in the main text and the reagents used are mentioned in the Supplementary Material. The data generated, used and/or analysed during the current study are available from the corresponding author on reasonable request.

#### REFERENCES

- Lennon, S., Oweida, A., Milner, D., Phan, A. V., Bhatia, S. & Van Court, B. et al. Pancreatic tumor microenvironment modulation by EphB4-ephrinB2 inhibition and radiation combination. *Clin. Cancer Res.* **25**, 3352–3365 (2019).
- Hazard, L. The role of radiation therapy in pancreas cancer. *Gastrointest Cancer Res.* **3**, 20–28 (2009).

3. Fogel, E. L., Shahda, S., Sandrasegaran, K., DeWitt, J., Easler, J. J. & Agarwal, D. M. et al. A multidisciplinary approach to pancreas cancer in 2016: a review. *Am. J. Gastroenterol.* **112**, 537–554 (2017).
4. Straub, J. M., New, J., Hamilton, C. D., Lominska, C., Shnyder, Y. & Thomas, S. M. Radiation-induced fibrosis: mechanisms and implications for therapy. *J. Cancer Res. Clin. Oncol.* **141**, 1985–1994 (2015).
5. Suklabaidya, S., Dash, P., Das, B., Suresh, V., Sasmal, P. K. & Senapati, S. Experimental models of pancreatic cancer desmoplasia. *Lab. Invest.* **98**, 27–40 (2018).
6. Yoshida, G. J., Azuma, A., Miura, Y., Orimo, A. Activated fibroblast program orchestrates tumor initiation and progression; molecular mechanisms and the associated therapeutic strategies. *Int. J. Mol. Sci.* **20**, 2256 (2019).
7. Magnusson, M., Högglund, P., Johansson, K., Jonsson, C., Killander, F. & Malmström, P. et al. Pentoxifylline and vitamin E treatment for prevention of radiation-induced side-effects in women with breast cancer: a phase two, double-blind, placebo-controlled randomised clinical trial (Ptx-5). *Eur. J. Cancer* **45**, 2488–2495 (2009).
8. Maier, P., Hartmann, L., Wenz, F., Herskind, C. Cellular pathways in response to ionizing radiation and their targetability for tumor radiosensitization. *Int. J. Mol. Sci.* **17**, 102 (2016).
9. Gunda, V., Souček, J., Abrego, J., Shukla, S. K., Goode, G. D. & Vernucci, E. et al. MUC1-mediated metabolic alterations regulate response to radiotherapy in pancreatic cancer. *Clin. Cancer Res.* **23**, 5881–5891 (2017).
10. Alexander, M. S., Wilkes, J. G., Schroeder, S. R., Buettner, G. R., Wagner, B. A. & Du, J. et al. Pharmacologic ascorbate reduces radiation-induced normal tissue toxicity and enhances tumor radiosensitization in pancreatic cancer. *Cancer Res.* **78**, 6838–6851 (2018).
11. Souček, J. J., Baine, M. J., Lin, C., Rachagani, S., Gupta, S. & Kaur, S. et al. Unbiased analysis of pancreatic cancer radiation resistance reveals cholesterol biosynthesis as a novel target for radiosensitization. *Br. J. Cancer* **111**, 1139–1149 (2014).
12. Kavalipati, N., Shah, J., Ramakrishnan, A. & Vasawala, H. Pleiotropic effects of statins. *Indian J. Endocrinol. Metab.* **19**, 554–562 (2015).
13. Lee, J. Y., Kim, M. S., Ju, J. E., Lee, M. S., Chung, N. & Jeong, Y. K. Simvastatin enhances the radiosensitivity of p53-deficient cells via inhibition of mouse double minute 2 homolog. *Int. J. Oncol.* **52**, 211–218 (2018).
14. Lacerda, L., Reddy, J. P., Liu, D., Larson, R., Li, L. & Masuda, H. et al. Simvastatin radiosensitizes differentiated and stem-like breast cancer cell lines and is associated with improved local control in inflammatory breast cancer patients treated with postmastectomy radiation. *Stem Cells Transl. Med.* **3**, 849–856 (2014).
15. Sanli, T., Liu, C., Rashid, A., Hopmans, S. N., Tsiang, E. & Schultz, C. et al. Lovastatin sensitizes lung cancer cells to ionizing radiation: modulation of molecular pathways of radioresistance and tumor suppression. *J. Thorac. Oncol.* **6**, 439–450 (2011).
16. Bourgier, C., Aupein, A., Rivera, S., Boisselier, P., Petit, B. & Lang, P. et al. Pravastatin Reverses Established Radiation-Induced Cutaneous and Subcutaneous Fibrosis in Patients With Head and Neck Cancer: Results of the Biology-Driven Phase 2 Clinical Trial Pravacur. *Int. J. Radiat. Oncol. Biol. Phys.* **104**, 365–373 (2019).
17. Haydout, V., Bourgier, C., Pocard, M., Lusinchi, A., Aigueperse, J. & Mathe, D. et al. Pravastatin Inhibits the Rho/CCN2/extracellular matrix cascade in human fibrosis explants and improves radiation-induced intestinal fibrosis in rats. *Clin. Cancer Res.* **13**, 5331–5340 (2007).
18. Ziegler, V., Henninger, C., Simantonakis, I., Buchholzer, M., Ahmadian, M. R. & Budach, W. et al. Rho inhibition by lovastatin affects apoptosis and DSB repair of primary human lung cells in vitro and lung tissue in vivo following fractionated irradiation. *Cell Death Dis.* **8**, e2978 (2017).
19. Li, J., Liu, J., Liang, Z., He, F., Yang, L. & Li, P. et al. Simvastatin and Atorvastatin inhibit DNA replication licensing factor MCM7 and effectively suppress RB-deficient tumors growth. *Cell Death Dis.* **8**, e2673 (2017).
20. Qi, X. F., Kim, D. H., Lee, K. J., Kim, C. S., Song, S. B. & Cai, D. Q. et al. Autophagy contributes to apoptosis in A20 and EL4 lymphoma cells treated with fluvastatin. *Cancer Cell Int.* **13**, 111 (2013).
21. Torres, M. P., Rachagani, S., Souček, J. J., Mallya, K., Johansson, S. L. & Batra, S. K. Novel pancreatic cancer cell lines derived from genetically engineered mouse models of spontaneous pancreatic adenocarcinoma: applications in diagnosis and therapy. *PLoS One* **8**, e80580 (2013).
22. Suklabaidya, S., Das, B., Ali, S. A., Jain, S., Swaminathan, S. & Mohanty, A. K. et al. Characterization and use of HapT1-derived homologous tumors as a preclinical model to evaluate therapeutic efficacy of drugs against pancreatic tumor desmoplasia. *Oncotarget* **7**, 41825–41842 (2016).
23. Das, B. & Senapati, S. Functional and mechanistic studies reveal MAGEA3 as a pro-survival factor in pancreatic cancer cells. *J. Exp. Clin. Cancer Res.* **38**, 294 (2019).
24. Westerfield, M., The zebrafish book. A guide for the laboratory use of zebrafish (*Danio rerio*). (Institute of Neuroscience, University of Oregon Press: Eugene, 2000)
25. Kimmel, C. B., Ballard, W. W., Kimmel, S. R., Ullmann, B. & Schilling, T. F. Stages of embryonic development of the zebrafish. *Dev. Dyn.* **203**, 253–310 (1995).
26. Henslee, A. B. & Steele, T. A. Combination statin and chemotherapy inhibits proliferation and cytotoxicity of an aggressive natural killer cell leukemia. *Biomark Res.* **6**, 26 (2018).
27. Alarcon Martinez, T., Zeybek, N. D. & Muftuoğlu, S. Evaluation of the cytotoxic and autophagic effects of atorvastatin on MCF-7 breast cancer cells. *Balkan Med. J.* **35**, 256–262 (2018).
28. Yang, L., Yang, G., Ding, Y., Dai, Y., Xu, S. & Guo, Q. et al. Inhibition of PI3K/AKT signaling pathway radiosensitizes pancreatic cancer cells with ARID1A deficiency in vitro. *J. Cancer* **9**, 890–900 (2018).
29. Bussink, J., van der Kogel, A. J. & Kaanders, J. H. Activation of the PI3-K/AKT pathway and implications for radioresistance mechanisms in head and neck cancer. *Lancet Oncol.* **9**, 288–296 (2008).
30. Naz, S., Sowers, A., Choudhuri, R., Wissler, M., Gamson, J. & Mathias, A. et al. Abemaciclib, a selective CDK4/6 inhibitor, enhances the radiosensitivity of non-small cell lung cancer in vitro and in vivo. *Clin. Cancer Res.* **24**, 3994–4005 (2018).
31. Qi, X. F., Zheng, L., Lee, K. J., Kim, D. H., Kim, C. S. & Cai, D. Q. et al. HMG-CoA reductase inhibitors induce apoptosis of lymphoma cells by promoting ROS generation and regulating Akt, Erk and p38 signals via suppression of mevalonate pathway. *Cell Death Dis.* **4**, e518 (2013).
32. Scripture, C. D. & Pieper, J. A. Clinical pharmacokinetics of fluvastatin. *Clin. Pharmacokinet.* **40**, 263–281 (2001).
33. Han, M. W., Lee, J. C., Choi, J. Y., Kim, G. C., Chang, H. W. & Nam, H. Y. et al. Autophagy inhibition can overcome radioresistance in breast cancer cells through suppression of TAK1 activation. *Anticancer Res.* **34**, 1449–1455 (2014).
34. Varshney, R., Varshney, R., Mishra, R., Gupta, S., Sircar, D. & Roy, P. Kaempferol alleviates palmitic acid-induced lipid stores, endoplasmic reticulum stress and pancreatic beta-cell dysfunction through AMPK/mTOR-mediated lipophagy. *J. Nutr. Biochem.* **57**, 212–227 (2018).
35. Parikh, A., Childress, C., Deitrick, K., Lin, Q., Rukstalis, D. & Yang, W. Statin-induced autophagy by inhibition of geranylgeranyl biosynthesis in prostate cancer PC3 cells. *Prostate* **70**, 971–981 (2010).
36. Zhang, J., Yang, Z., Xie, L., Xu, L., Xu, D. & Liu, X. Statins, autophagy and cancer metastasis. *Int. J. Biochem. Cell Biol.* **45**, 745–752 (2013).
37. Zhu, Z., Zhang, P., Li, N., Kiang, K. M. Y., Cheng, S. Y. & Wong, V. K. et al. Lovastatin enhances cytotoxicity of temozolomide via impairing autophagic flux in glioblastoma cells. *Biomed. Res. Int.* **2019**, 2710693 (2019).
38. Cunha, V., Santos, M. M., Moradas-Ferreira, P., Castro, L. F. C. & Ferreira, M. Simvastatin modulates gene expression of key receptors in zebrafish embryos. *J. Toxicol. Environ. Health A* **80**, 465–476 (2017).
39. Zhang, H., Yue, J., Jiang, Z., Zhou, R., Xie, R. & Xu, Y. et al. CAF-secreted CXCL1 conferred radioresistance by regulating DNA damage response in a ROS-dependent manner in esophageal squamous cell carcinoma. *Cell Death Dis.* **8**, e2790 (2017).
40. Liu, Q., Wang, M., Kern, A. M., Khaled, S., Han, J. & Yeap, B. Y. et al. Adapting a drug screening platform to discover associations of molecular targeted radiosensitizers with genomic biomarkers. *Mol. Cancer Res.* **13**, 713–720 (2015).
41. Doi, H., Matsumoto, S., Odawara, S., Shikata, T., Kitajima, K. & Tanooka, M. et al. Pravastatin reduces radiation-induced damage in normal tissues. *Exp. Ther. Med.* **13**, 1765–1772 (2017).
42. Bocci, G., Fioravanti, A., Orlandi, P., Bernardini, N., Collecchi, P. & Del Tacca, M. et al. Fluvastatin synergistically enhances the antiproliferative effect of gemcitabine in human pancreatic cancer MIAPaCa-2 cells. *Br. J. Cancer* **93**, 319–330 (2005).
43. Efimova, E. V., Ricco, N., Labay, E., Maucri, H. J., Flor, A. C. & Ramamurthy, A. et al. HMG-CoA reductase inhibition delays dna repair and promotes senescence after tumor irradiation. *Mol. Cancer Ther.* **17**, 407–418 (2018).
44. Marechal, A., Zou, L. DNA damage sensing by the ATM and ATR kinases. *Cold Spring Harb. Perspect. Biol.* **5**, a012716 (2013).
45. Pali, S. S., Cui, Y., Innes, C. L. & Paules, R. S. Dissecting cellular responses to irradiation via targeted disruptions of the ATM-CHK1-PP2A circuit. *Cell Cycle* **12**, 1105–1118 (2013).
46. Gobbini, E., Cesena, D., Galbiati, A., Lockhart, A. & Longhese, M. P. Interplays between ATM/Tel1 and ATR/Mec1 in sensing and signaling DNA double-strand breaks. *DNA Repair.* **12**, 791–799 (2013).
47. Yang, Z., Su, Z., DeWitt, J. P., Xie, L., Chen, Y. & Li, X. et al. Fluvastatin prevents lung adenocarcinoma bone metastasis by triggering autophagy. *EBioMedicine* **19**, 49–59 (2017).
48. Apel, A., Herr, I., Schwarz, H., Rodemann, H. P. & Mayer, A. Blocked autophagy sensitizes resistant carcinoma cells to radiation therapy. *Cancer Res.* **68**, 1485–1494 (2008).
49. Classen, F., Kranz, P., Riffkin, H., Pomsch, M., Wolf, A. & Gopelt, K. et al. Autophagy induced by ionizing radiation promotes cell death over survival in human colorectal cancer cells. *Exp. Cell Res.* **374**, 29–37 (2019).
50. Wang, F., Tang, J., Li, P., Si, S., Yu, H. & Yang, X. et al. Chloroquine enhances the radiosensitivity of bladder cancer cells by inhibiting autophagy and activating apoptosis. *Cell Physiol. Biochem.* **45**, 54–66 (2018).

## ACKNOWLEDGEMENTS

We sincerely thank Dr. Soumen Chakraborty, Institute of Life Sciences for his help in utilizing the radiation facility. We are thankful to Dr. Naresh Bal (KIIT University, Bhubaneswar) for his valuable suggestions and comments. We thank Mr. Madan Mohan Mallick, and Mr. Sushanta Kumar Swain, for their efficient technical support. We acknowledge the Director, Institute of Life Sciences for supporting the project.

## AUTHOR CONTRIBUTIONS

Conception, design and development of methodology, data analysis and interpretation: S.S., D.M., V.S., and B.D. Experiments associated with zebrafish experiment: D.M., D.P., U.N., R.K.S., S.S. Writing, review, and/or revision of the manuscript: D.M., S.S., B.D., V.S., A.P.M., and D.M. Study supervision: S.S.

## FUNDING

The study was supported by Institute of Life Sciences and Department of Biotechnology, Government of India.

## COMPETING INTERESTS

The authors declare no competing interests.

## ETHICS APPROVAL

All animal experimental procedures were approved by the Animal Ethics Committee of Institute of Life Sciences, India.

## ADDITIONAL INFORMATION

**Supplementary information** The online version contains supplementary material available at <https://doi.org/10.1038/s41374-021-00690-7>.

**Correspondence** and requests for materials should be addressed to Shantibhusan Senapati.

**Reprints and permission information** is available at <http://www.nature.com/reprints>

**Publisher's note** Springer Nature remains neutral with regard to jurisdictional claims in published maps and institutional affiliations.